Preparation of Nanocrystalline TiO2 Electrodes for Flexible Dye-Sensitized Solar Cells: Influence of Mechanical Compression

ARTICLE *in* THE JOURNAL OF PHYSICAL CHEMISTRY C · SEPTEMBER 2012

Impact Factor: 4.77 · DOI: 10.1021/jp301638p

4 AUTHORS:

Senthilarasu Sundaram
University of Exeter
64 PUBLICATIONS **757** CITATIONS
SEE PROFILE

T. A. Nirmal Peiris
The University of Tokyo
17 PUBLICATIONS **82** CITATIONS
SEE PROFILE

Jorge García-Cañadas
Universitat Jaume I
36 PUBLICATIONS **502** CITATIONS
SEE PROFILE

K. G. Upul Wijayantha
Loughborough University
87 PUBLICATIONS **3,440** CITATIONS
SEE PROFILE

THE JOURNAL OF PHYSICAL CHEMISTRY C

Article

pubs.acs.org/JPCC

Preparation of Nanocrystalline TiO_2 Electrodes for Flexible Dye-Sensitized Solar Cells: Influence of Mechanical Compression

S. Senthilarasu,[†] T. A. Nirmal Peiris,[†] Jorge García-Cañadas,[‡] and K. G. Upul Wijayantha*[,†]

[†]Department of Chemistry, Loughborough University, Loughborough, Leics, LE11 3TU, United Kingdom

[‡]Cardiff School of Engineering, Cardiff University, The Parade, Cardiff, CF24 3AA, United Kingdom

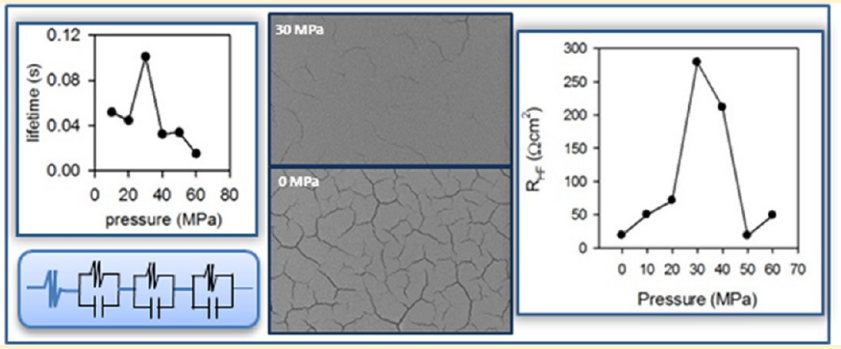

ABSTRACT: Nanocrystalline TiO_2 electrodes were prepared using binder-free TiO_2 paste on conductive ITO-PEN substrates by the doctor-blade method at significantly low temperature (140 °C), and the electrodes were further processed under different compressions (10−60 MPa) in order to improve interparticle connections and adhesion between the nanoparticles and the ITO-PEN substrate. TiO_2 electrodes compressed at 30 and 40 MPa had relatively less cracks with low crack width. Electrode compressed at 30 MPa showed the highest internal surface area. Electrode prepared at this compression showed the best dye-sensitized solar cell (DSC) performance with V_{oc} of 805 mV, J_{sc} of 9.24 mA cm^{-2}, and an overall efficiency of 4.39%. Electrochemical impedance spectroscopy (EIS) studies of the sandwiched cells employing bare nanocrystalline TiO_2 electrode and Pt counter electrode in I^-/I_3^- electrolyte showed that electrode compression significantly influences the stability of the cells. EIS data suggested that degradation/corrosion processes may take place on ITO-PEN for sandwiched cells made by TiO_2 electrodes compressed at all pressures. Thirty and 40 MPa compressions showed a minor degradation of ITO. The recombination dynamics at the TiO_2/electrolyte interface were influenced by the changes in the nanostructured electrode internal surface area, changes in electron transport properties (due to improved sintering), and possible degradation/corrosion of ITO-PEN. Open-circuit voltage decay (OCVD) measurements showed that the DSC made by the 30 MPa compressed TiO_2 electrode had the highest decay time, indicating low recombination properties, which is in a good agreement with other data.

1. INTRODUCTION

There has been a recent surge of interest in flexible solar cells due to a wide range of new and emerging applications such as mobile power for wearable electronic devices. Construction of flexible DSCs, in particular, has attracted significant attention due to low production cost.[1,2] Nanocrystalline TiO_2 electrode, which is a key component of rigid DSC, is typically prepared by screen printing or the doctor-blade technique on conductive FTO glass substrates using titania paste containing an organic binder, followed by an annealing step at 450−500 °C in air.[3] The relatively high-temperature sintering step is necessary to burn off the organic binders, to fuse individual TiO_2 nanoparticles (to ensure an electrical passage), and to establish electrical contact between TiO_2 and FTO coating on glass substrate. However, the sintering step at 450−500 °C cannot be directly adopted for preparation of TiO_2 electrode on flexible substrate in the flexible DSC construction. The poor thermal stability of currently available conductive and transparent flexible substrates (i.e., PET, PEN) precludes sintering at 450−500 °C, thereby prohibiting the use of organic binder-based pastes for deposition of nanocrystalline TiO_2 electrodes on plastic substrates. Even in the case of use of binder-free TiO_2 paste to prepare nanocrystalline electrode on flexible substrates, alternative low-temperature treatments are thus required in order to improve the connectivity between individual TiO_2 nanoparticles as well as between TiO_2 and ITO.

In order to tackle this issue, low-temperature compression methods have been developed.[2,4] DSCs constructed from TiO_2 electrodes prepared by both mechanical compression[4] and chemical sintering[5] have shown promising power conversion efficiencies on the order of 7%. A recent study[6] shows the influence of compression in the DSC performance, but it is based on a binder-free titania paste made up of a mixture of different nanoparticle sizes, which complicates nanoporous film

Received: February 19, 2012
Revised: July 27, 2012
Published: August 8, 2012

preparation. Besides, that particular study does not cover the impedance studies in the whole voltage range, where crucial information (i.e., recombination, energetics of the cells, degradation processes, etc.) can be deduced. Furthermore, there is a lack of systematic studies to date to understand the low-temperature compression method and its merits and drawbacks on key DSC parameters that determine the cell performance. This highlights the urgent need of further studies in this area to understand the influence of compression on the internal processes of the cells and determine the most suitable electrode preparation conditions for efficient DSC construction.

We recently studied the surface coating of nanocrystalline TiO_2 electrodes (prepared on flexible ITO-PEN substrates) with $Mg(OH)_2$ by electrodeposition and its influence on DSC performance.[2] In that case, TiO_2 electrodes were prepared using binder-free paste on flexible substrate and compressed at 30 MPa. In the present work, we systematically investigated the influence of mechanical compression in TiO_2 electrode preparation on the performance of flexible DSCs. Nanocrystalline TiO_2 electrodes were prepared by applying different mechanical compressions ranging from 10 to 60 MPa. Effects of mechanical compression on the internal processes taking place in the cells were evaluated by conducting electrochemical impedance spectroscopy (EIS) studies and open-circuit voltage decay (OCVD) measurements for sandwiched cells containing a bare TiO_2 electrode and a Pt counter electrode. Findings of this study will have a direct impact on the ongoing work on development of flexible DSCs. In addition, the outcome of this work will also be beneficial in the construction of plastic electronic devices in general.

2. EXPERIMENTAL METHODS

Nanocrystalline TiO_2 electrodes were prepared from a binder-free colloidal suspension of TiO_2 (P-25, Degussa) nanoparticles. Colloidal suspension was dispersed on the ITO-PEN substrates (13 Ω/□, Peccell Technologies, Inc., Japan) by the doctor-blade method. TiO_2-coated ITO-PEN substrates were then heated at 140 °C for 30 min on a hot plate.[7] The resulting electrodes were compressed by a static mechanical press (10 MPa ≤ compression ≤ 60 MPa). Surface morphology of the nanocrystalline TiO_2 electrodes was studied using a Leo 1530 VP field emission gun scanning electron microscope (FEG-SEM) at an accelerating voltage of 5 kV and a working distance of 5 mm.

The compressed nanocrystalline TiO_2 electrodes were soaked overnight in an ethanolic solution of 1×10^{-6} M N719 dye (*cis*-diisothiocyanato-bis(2,2′-bipyridyl-4,4′-dicarboxylato)ruthenium(II) bis(tetrabutylammonium)) (Solaronix SA), sandwiched with a platinized conducting counter electrode prepared on ITO-PEN substrate using a Surlyn frame (Solaronix SA), filled with electrolyte through a hole in the counter electrode, and sealed. The iodide/tri-iodide electrolyte comprising 0.4 M LiI, 0.4 M tetrabutylammonium iodide (TBAI), and 0.04 M I_2 dissolved in 0.3 M *N*-methylbenzimidazole (NMB) in acetonitrile (ACN) and 3-methoxypropionitrile (MPN) solvent mixture at a volume ratio of 1:1 was used. The area of the cells was 0.25 cm^2. The internal surface area of the TiO_2 electrodes was estimated by conducting dye adsorption/desorption measurements.[2] The concentration of desorbed dye in a 0.1 M NaOH solution was recorded by measuring the absorbance (Lambda 35 Perkin-Elmer UV−vis spectrometer). Prior to recording the absorbance spectra, the solution was acidified by adding an appropriate amount of 0.1 M aqueous HCl solution.

Steady-state current−voltage measurements of the cells were carried out using a potentiostat (Eco Chemie micro-Autolab type III), while the cells were illuminated using an AM 1.5 Class A solar simulator (Solar Light 16S-300 solar simulator) at 100 mW cm^{-2} light intensity, calibrated by a silicon pyranometer (Solar Light Co., PMA2144 Class II). Incident photon to electron conversion efficiency (IPCE) measurements were conducted using a 75 W xenon lamp connected to a monochromator (Bentham, TMc300), and the system was calibrated using a UV-enhanced silicon photodiode (Bentham). IPCE spectra of DSCs were recorded while the cells were illuminated through the substrate side over the 300−800 nm spectral range using a chopping frequency of 5 Hz.

Electrochemical impedance spectroscopy studies and OCVD measurements were carried out for cells made with compressed nanocrystalline TiO_2 electrodes (10−60 MPa) using a standard potentiostat (micro-Autolab, type III) equipped with a frequency response analyzer. Impedance measurements were carried out under different applied potentials between 0 and −0.9 V in steps of 0.1 V in the dark. The amplitude of the ac signal used was 10 mV, and the frequency range was 10^{-2}−10^6 Hz. Recorded spectra were fitted with Z-View software (v3.2d, Scribner Associate, Inc., USA) using appropriate equivalent circuits. For OCVD measurements, cells were illuminated with white light at 100 mW cm^{-2} intensity until the photovoltage was stabilized. Then the light was turned off, and the open-circuit voltage was recorded at 50 ms intervals.

3. RESULTS AND DISCUSSION

3.1. Compressed Flexible Nanocrystalline TiO_2 Electrodes. Cracks occurring in electrodes during the drying step of wet electrodes are well known.[8] When a solvent-based particle suspension is used to prepare a thin film electrode through a printing process (i.e., screen printing, doctor blade), if the solvent is allowed to evaporate from the paste at room temperature, then the solid suspension will undergo a series of transformations and finally form a dry electrode. The mechanism of this transformation is described in different ways.[8] It is generally accepted that the transformation of a solid suspension to a dry electrode takes place via four main stages as described: stage I, dispersed suspension of solid particles; stage II, concentrated suspension of particles in contact with each other, surrounded by solvent-filled interstices; stage III, continuous ordered array of particles deformed by van der Waals and capillary forces; and stage IV, continuous electrode formed as a result of diffusion of particles.[9] Cracks appear when wet electrodes are dried, and their size is determined by the environment, ink formulation, and thickness of the coating.

Therefore, it is important to understand the mechanism by which an electrode can be successfully prepared from a paste without cracks and other deformations. A number of mechanisms have been proposed as discussed below. Studies suggest that formation of cracks is generally caused by shrinkage of materials at stage III. According to Jagla et al.,[10] in the case of use of an aqueous suspension, shrinking is due to changes in the humidity concentration inside the material and nonuniform distributions of temperature. Lee and Routh[11] suggested that crack formation is due to the particle agglomeration during the drying process of wet inks. As Lan et al.[12] stated, the cracks may be caused by the residual stress between the settled and the packed particles in the drying

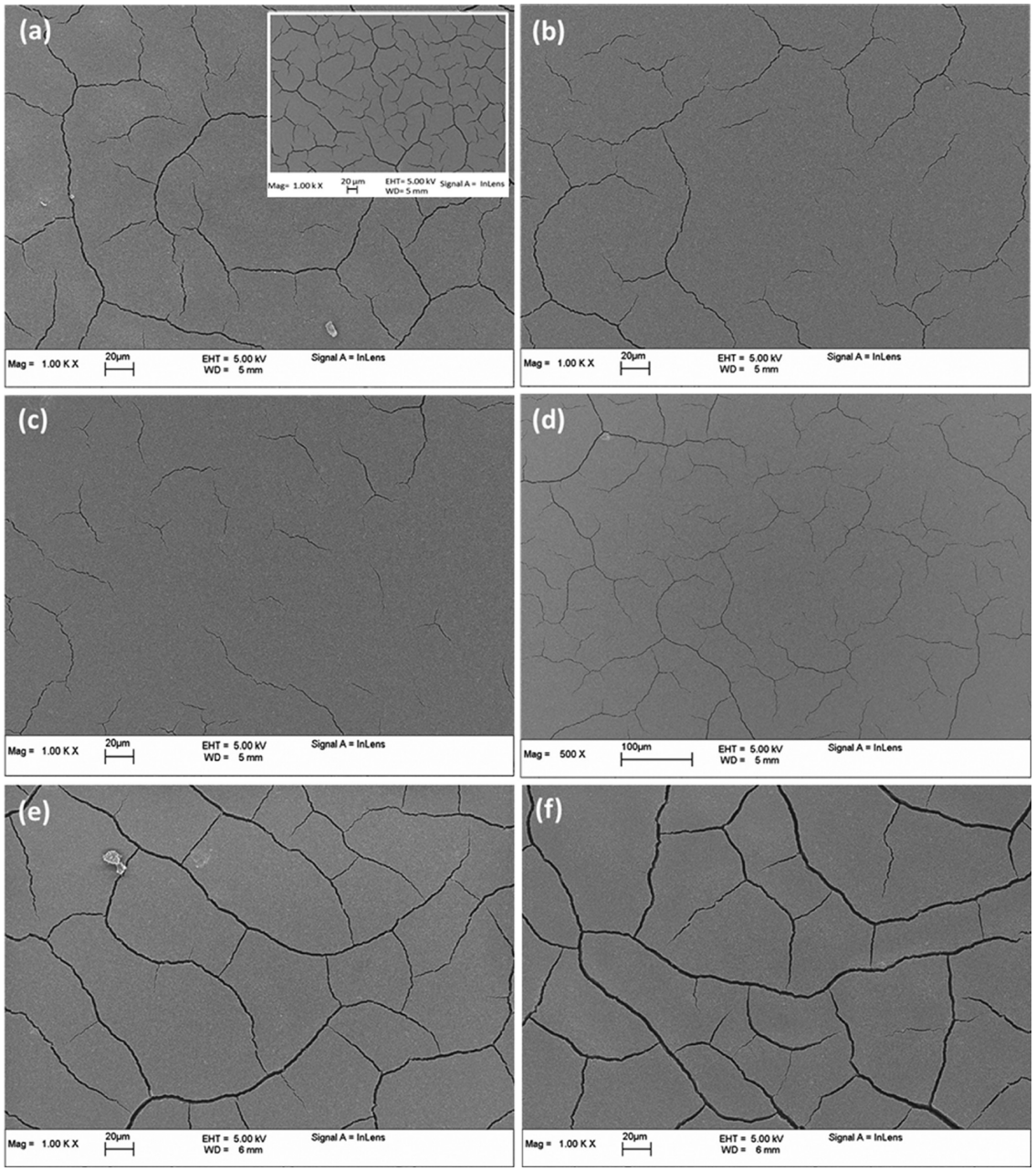

Figure 1. Topographical FEG-SEM images of nanocrystalline TiO_2 electrodes prepared as the mechanical compression is systematically varied: (a) 10, (b) 20, (c) 30, (d) 40, (e) 50, and (f) 60 MPa. (Inset) Surface topographical image of the TiO_2 electrode without compression at the same magnification and scale as in (a).

process. Other studies suggest that cracks usually initiate at surface defects (large aggregate anomalies, small topographic features, indentations, etc.).[13] Hence, generally cracks are more prominent in binder-free TiO_2 electrodes, especially when they are fabricated using low-temperature techniques.

Figure 1a–f shows the FEG-SEM topography of the TiO_2 electrodes prepared as mechanical compression is systematically increased from 10 to 60 MPa.

Drying of the wet ethanolic TiO_2 film starts when the solvent–air interface reaches the TiO_2 surface, forming an ethanol–air meniscus between TiO_2 nanoparticles, which eventually leads to developing a capillary suction in the upper layer of the TiO_2 wet electrode. As solvent evaporation proceeds, the curvature of capillary meniscus is increased and accompanied by an increase of capillary suction and effective stress between TiO_2 nanoparticles. Consequently, the TiO_2 layer consolidates and shrinks. From the particle level, each particle in the surface layer suffers a tensile force, which is induced by the capillary suction developed from the surrounded particles. Therefore, a tensile stress field is set up in the upper layer. Once the rising tensile stress exceeds the tensile strength of the TiO_2 layer, cracking occurs on the surface.[14]

In the present study, a number of reasons may have directly influenced crack formation during the drying step of TiO_2 electrodes preparation, such as rapid evaporation of ethanol, changes in the capillary forces, reduction in the bonding strength among TiO_2 particles, and a mismatch of the thermal expansion between the substrate and the wet electrode.[15] A typical TiO_2 electrode is initially dried at room temperature and

dx.doi.org/10.1021/jp301638p | J. Phys. Chem. C 2012, 116, 19053–19061

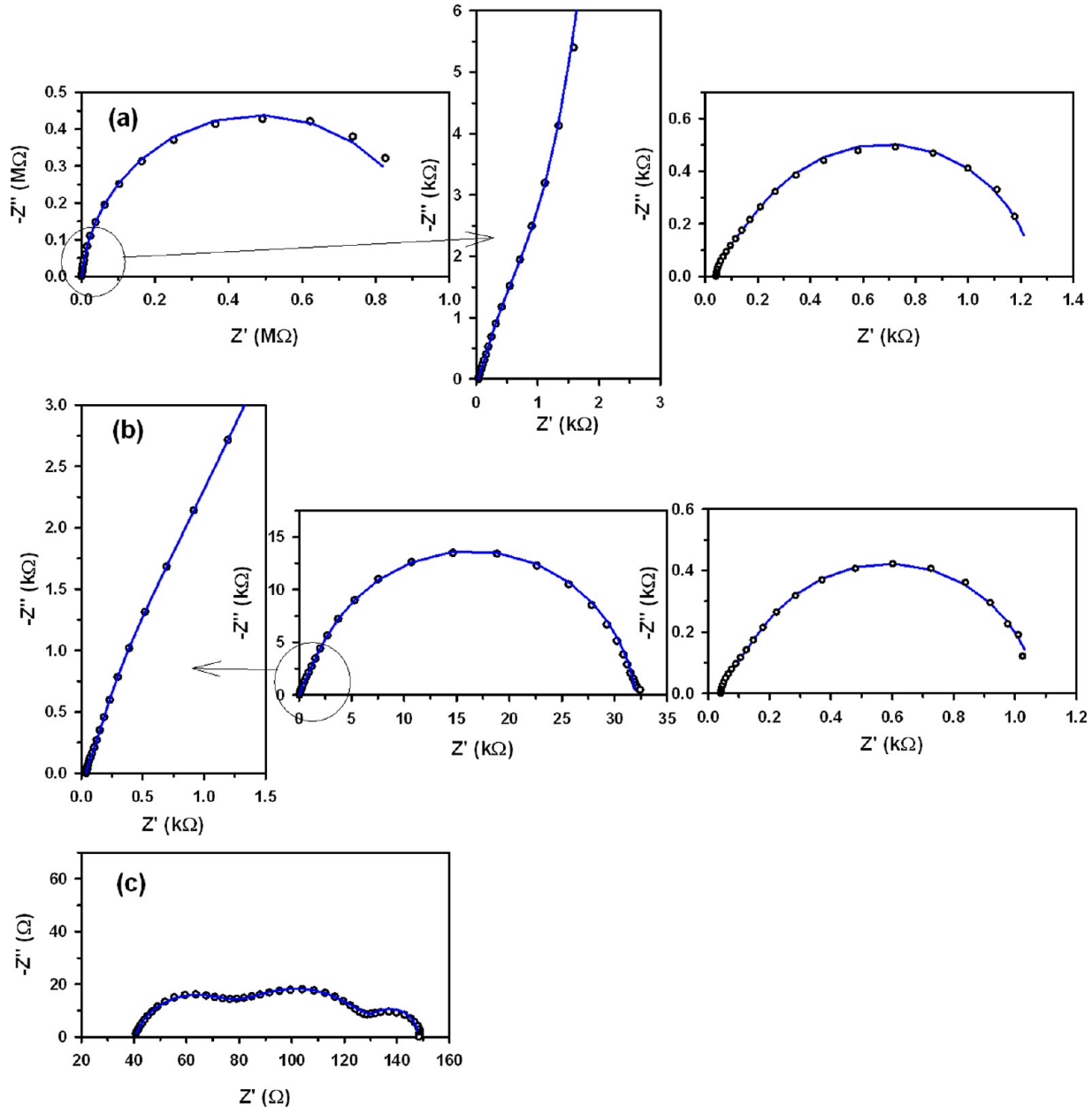

Figure 2. Dark impedance spectra (dots) of the complete cells constructed with TiO_2 electrodes compressed at 30 MPa at applied voltages of (a) −0.2, (b) −0.4, and (c) −0.8 V. Enlarged segments at high frequency are displayed in a and b, and plot on the right is the result of subtracting the low-frequency (right) semicircle, which clarifies the existence of three semicircles. Fitted data are shown in the blue line.

further dried on a surface of a hot plate at 140 °C prior to mechanical compression. Ethanol in the wet electrode evaporates at an increased rate at 140 °C; also, the low density of solid in the wet coating may enhance evaporation of ethanol, hence creating a steep difference of the tensile strengths in the bulk and upper layer, which leads to crack formation in the electrode. Yamaguchi et al.[7] studied the role of heat treatment in the compression method on flexible DSC. They measured the performance of electrodes which were compressed without heating and electrodes which were subjected to heat treatment before compression. It was found that despite the presence of cracks in the heat-treated film, this only slightly diminishes the performance and no relevant differences were observed. However, applying a mechanical compression on the electrode brings individual TiO_2 nanoparticles together, thereby increasing the packing density, resulting in fewer cracks.[15] At low compression (i.e., 10 MPa), nanoparticle segregation on dried electrodes is induced by filling the voids of the nanoporous electrodes by particle movements. Further increase of the mechanical compression up to 40 MPa improves the electrical connections between individual TiO_2 nanoparticles as well as between TiO_2 and ITO-PEN. When compression was increased further (>40 MPa) the orderly packing of TiO_2 nanoparticles in the electrode matrix was disturbed and eventually collapsed (Figure 1). This may have caused reappearing of cracks in the electrodes at relatively high compressions.[16]

3.2. EIS Measurements of Sandwiched TiO_2 Cells. In order to understand the influence of mechanical compression on the internal processes of the sandwiched cells, EIS measurements were performed in the dark. Figure 2 shows the evolution of the impedance spectra of a sandwiched cell

(made by TiO_2 electrode compressed at 30 MPa) at different applied voltages and corresponding data fittings. The sandwiched cells constructed using electrodes prepared at other compressions also showed a similar trend (data not shown). Figure 3a illustrates the general equivalent circuit for a DSC.[17] EIS spectra have been fitted using the equivalent circuits in Figure 3b and 3c. Constant phase elements (CPEs) instead of pure capacitors were employed as they describe the nonideal response of the cells better. The features of the spectra depend on the voltage range and are not always equivalent at all pressures. In general, we can define three different ranges: (i) at more positive voltages (from −0.4 to 0 V) the EIS responses are characterized by three overlapped semicircles appearing in the high- (left), medium- (middle), and low-frequency (right) ranges (Figure 2a), which are fitted using the equivalent circuit given in Figure 3b. We should remark that for the cells made using 30, 40, and 50 MPa mechanical compressions, this trend is extended up to −0.6 V. In this range the nanostructured electrode is poorly conductive. The right arc is related to recombination at the ITO/electrolyte interface, the middle semicircle is not usually observed in spectra of glass-based sandwiched TiO_2, and the left semicircle is attributed to the Pt/electrolyte interface, although some other contributions may exist as we will discuss later. This semicircle is also present in the rest of the voltage ranges. (ii) At medium voltages (from −0.6 to −0.5 V) the spectra display two semicircles, which has been fitted using the equivalent circuit of Figure 3c excluding the diffusion element (Z_d). Here the electrical conductivity of the porous TiO_2 network starts to increase due to charge accumulation and the processes occurring at the TiO_2/electrolyte interface are predominant and described by the low-frequency (right) semicircle. (iii) At more negative voltages (from −0.9 to −0.7 V), the diffusion element (Z_d) accounting for diffusion of redox species appeared at low frequency (right) in addition to the two semicircles and the spectra was fitted using the complete circuit of Figure 3c. The usual feature attributed to electronic transport resistance in the TiO_2 electrode (i.e., ∼45° slope) has not been clearly observed in the spectra (Figure 2b) since it is overlapped with other processes (i.e., middle semicircle and/or ITO/TiO_2 contact resistance).

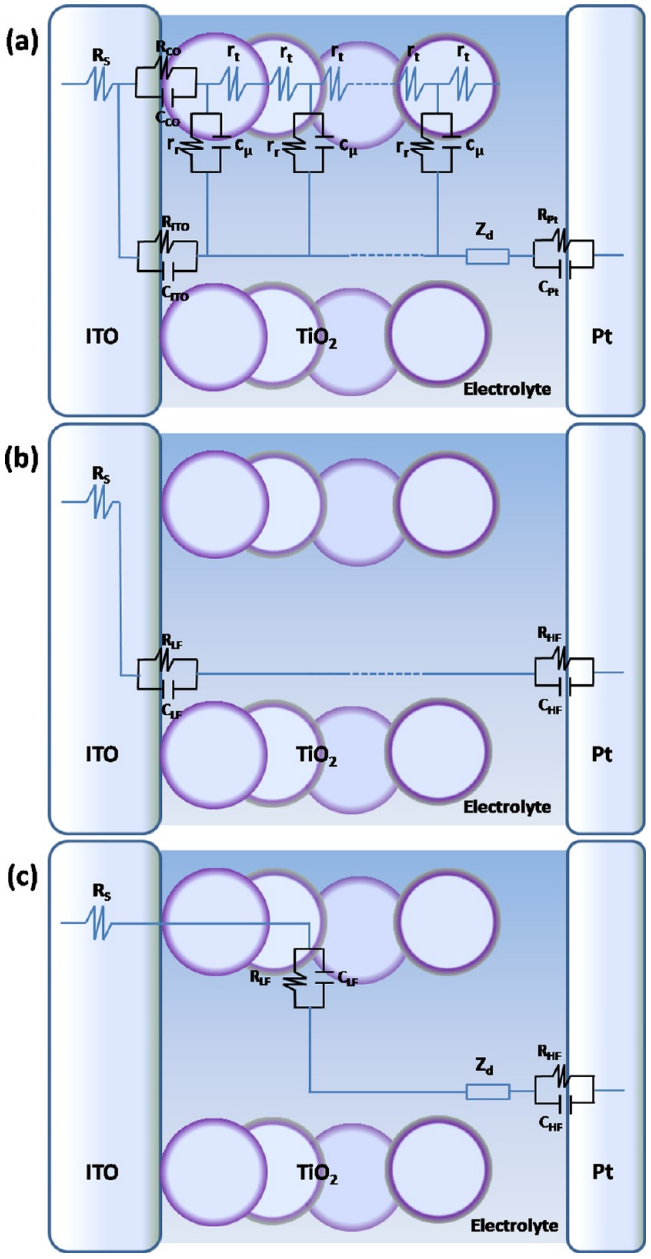

Figure 3. Equivalent circuits for DSC. (a) General equivalent circuit. Simplified circuits used for data fitting at (b) more positive potentials and (c) more negative potentials. R_s is the series resistance, R_{CO} and C_{CO} account for the ITO/TiO_2 contact connection, R_{ITO} and C_{ITO} describe the recombination process at the ITO/electrolyte interface, r_t, r_r, and c_μ are the microscopic electronic transport resistance, recombination resistance, and chemical capacitance from TiO_2, respectively. R_r and C_μ are the macroscopic recombination resistance and chemical capacitance. Z_d accounts for diffusion of the redox species, and R_{Pt} and C_{Pt} describe the charge transfer from the Pt counter electrode/electrolyte interface. R_{LF}, C_{LF}, R_{MF}, C_{MF}, R_{HF}, and C_{HF} describe in general the low-, medium-, and high-frequency responses, respectively.

Figure 4a describes the resistance at high frequencies (R_{HF} from the left semicircle) against the applied voltage at different compressions for the sandwiched cells, which extends over the whole voltage range. In the positive applied voltages (from −0.4 to 0 V), the R_{HF} is almost constant. A similar trend has been reported for glass-based DSC, where this response is due to the charge transfer resistance at the counter electrode (R_{Pt}).[17] However, the observed R_{HF} from the compressed electrodes is higher than R_{Pt}, which is deduced from data of the cell with noncompressed electrode (0 MPa). When electrons start to accumulate in the TiO_2 at −0.5 V, the R_{HF} drastically dropped down to the minima except for the noncompressed electrode. This suggests that another process may be occurring in addition to the ITO-PEN counter electrode response. This unusual behavior is influenced by compression and fades away when TiO_2 becomes conductive. At voltages negative to −0.6 V, R_{HF} values of the compressed cells showed behavior similar to the Pt/electrolyte response (cell with noncompressed TiO_2). The nature of the R_{HF} behavior is not completely understood, but we believe that it could be due to degradation or corrosion that may be undergoing at the ITO-PEN substrate, which has been reported by others previously.[18−20] Damage caused at the substrate due to compression (during the electrode construction stage) has been evidenced by SEM studies conducted for substrates once the TiO_2 film is carefully detached (not shown). Figure 4b indicates the variation of R_{HF} against compression at −0.2 V. The highest R_{HF} values corresponding to 30 and 40 MPa compressions under the assumption of being

dx.doi.org/10.1021/jp301638p | J. Phys. Chem. C 2012, 116, 19053−19061

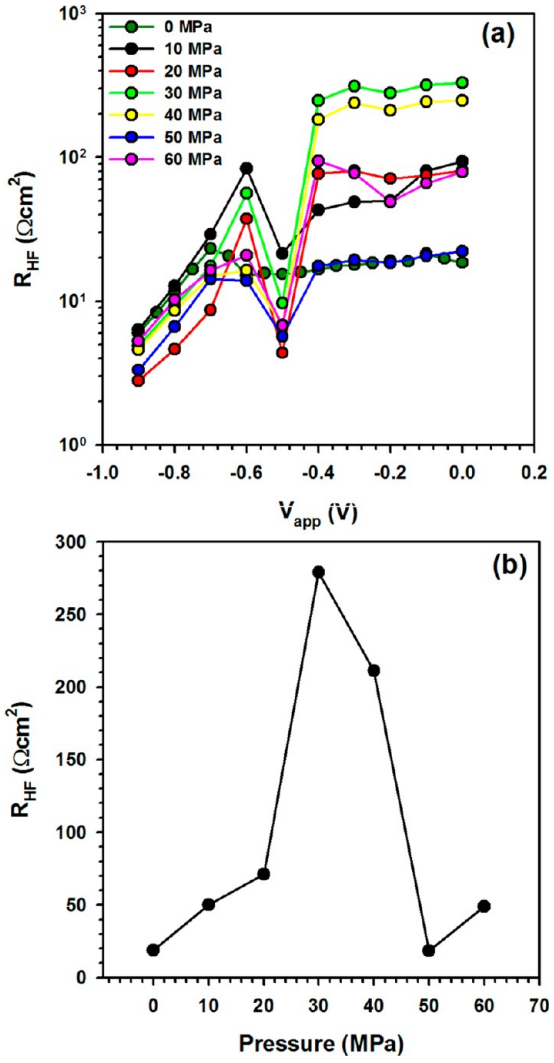

Figure 4. (a) High-frequency resistance response of the cells in the dark versus the applied voltage at the different compressions. (b) Variations of the high-frequency resistance at −0.2 V with electrode compression.

a degradation process suggest a minor degradation occurring in the ITO substrate (R_{HF} accounts for the kinetics of the reaction). As described in Figure 1c and 1d, the electrodes prepared at 30 and 40 MPa showed fewer cracks with reduced crack width compared to the electrodes prepared at other compressions. Therefore, it appears that the force exerted by compression particularly at 30 and 40 MPa is inverted in the nanoparticle sintering instead of stressing the substrate.

At the medium-frequency regime a middle semicircle is observed in the more positive voltage range for all cells except for the cell made with the noncompressed electrode. Usually this is related to the ITO/TiO_2 interfacial or corrosion events,[19] which are not common in glass-based rigid DSCs. Figure 5 shows the variation of the resistance of the middle semicircle (R_{MF}) of the cells with the applied compression on the TiO_2 electrodes. The R_{MF} is constant for the applied voltage above −0.4 V. This semicircle disappeared at voltages negative to −0.4 V, except for 30−50 MPa compressed electrodes in which case an increase of R_{MF} is observed. This could be due to the overlapping of the transport resistance (r_r) and/or the ITO/TiO_2 contact resistance (R_{CO}). The nature of this event is not

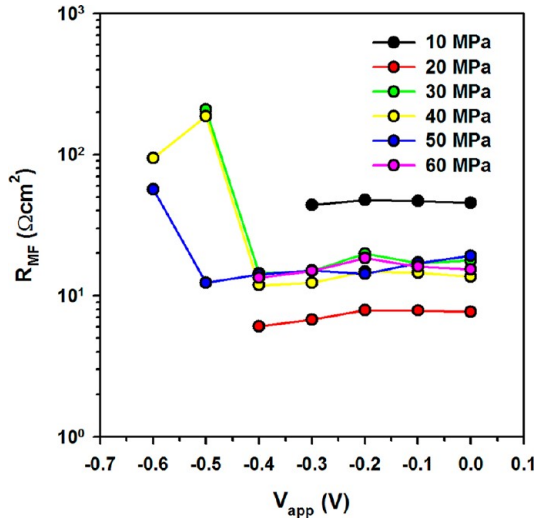

Figure 5. Medium-frequency resistance deduced from impedance data of the cells in the dark constructed with TiO_2 electrodes prepared at different compressions.

very clear, and we believe that this could be due to degradation or corrosion of ITO-PEN.[20]

The recombination processes and accumulation of charges in the photoelectrode are given by the recombination resistance (R_{rec}) and the cell capacitance (C_{cell}), respectively. At voltages more positive than −0.4 V recombination from the ITO-PEN (R_{LF}, C_{LF}) is predominant, and at more negative voltages recombination from the TiO_2/electrolyte interface dominates (R_r, C_μ). Figure 6 shows the variation of R_{rec} and C_{cell} of the cells made by the electrode prepared at different compressions as a function of applied voltage. Both vary several orders of magnitude along the voltage range considered, as observed in glass-based DSCs.[21] From the onset of the C_{cell} (Figure 6b), it can be seen that the cells follow the same energetics, indicating that the position of the conduction band of TiO_2 does not change against the degree of compression in TiO_2 electrode preparation. At −0.5 V the electrons start to accumulate in the nanostructured electrode, raising C_{cell}, and recombination starts to take place from the TiO_2 nanoparticles. Due to the changes that may occur in electrode porosity and thickness at different compressions, the electron lifetime is compared.[22] Electron lifetime is calculated by taking the product of the recombination resistance (R_{rec}) and the cell capacitance (C_{cell}). Figure 6c shows that there is no significant change in the electron lifetime of the cells at voltages more positive than −0.4 V. This indicates that the area of ITO substrate exposed to the electrolyte (i.e., ITO uncoated with TiO_2) is almost the same for all sandwiched cells and has not been influenced by the different compressions applied in the electrode preparation. At voltages negative to −0.4 V, recombination through the nanocrystalline TiO_2 electrodes becomes predominant and no significant changes are observed for different compressions. Dye adsorption/desorption studies confirmed that the internal surface area of TiO_2 increases with compression up to 30 MPa and then decreases again (Table 1), showing the highest internal surface area for the electrode compressed at 30 MPa. However, this is not reflected in the recombination properties (Figure 6c). This may be due to the fact that surface area enhancement is counter balanced by efficient charge collection as the charge transport properties of TiO_2 may have increased with improved sintering (as suggested by FEG-SEM studies).

dx.doi.org/10.1021/jp301638p | J. Phys. Chem. C 2012, 116, 19053−19061

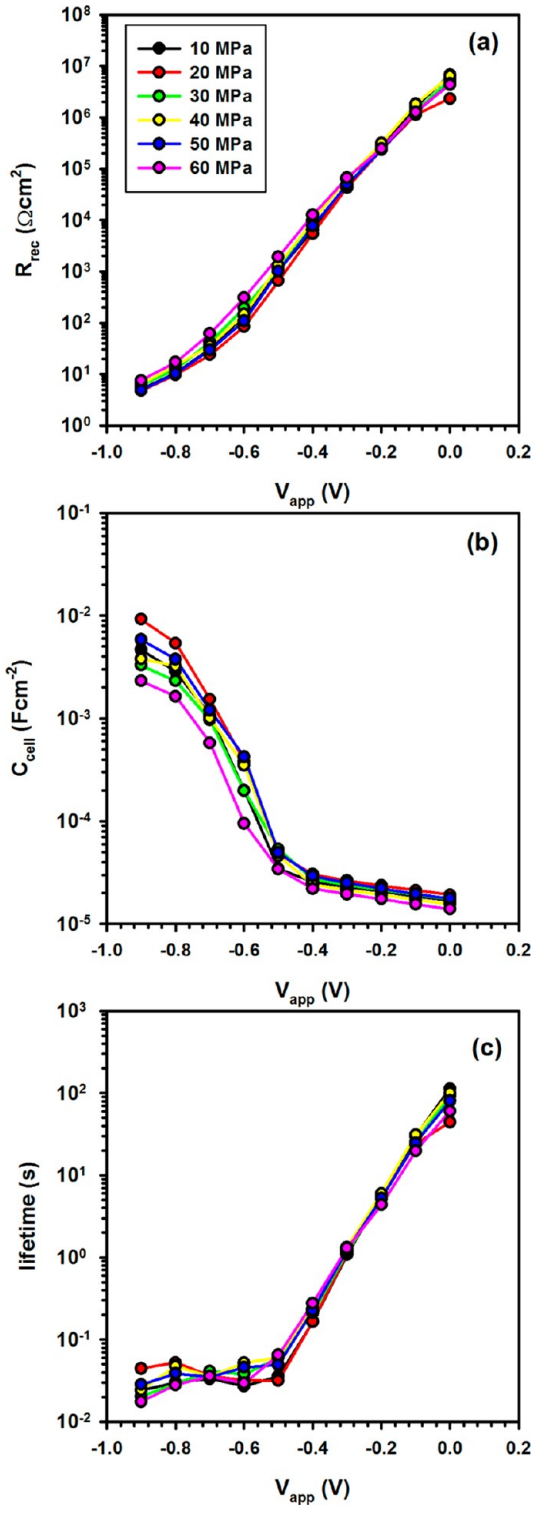

Figure 6. Impedance response at low frequencies in the dark as a function of applied voltage for cells made using TiO_2 electrodes prepared at different compressions: (a) recombination resistance, (b) cell capacitance, and (c) electron lifetime.

In addition, ITO-PEN corrosion is relatively low at 30 and 40 MPa and supports this observation. Unfortunately, no information on charge transport can be extracted from the impedance measurements, since they are hidden by other processes. Although a combination of EIS and intensity-modulated photocurrent spectroscopy (IMPS) can be used to deduce transport information,[23] such study is beyond the scope of the present work and will be considered in a dedicated work later.

Table 1. Key Cell Parameters of DSCs Made with TiO_2 Electrodes Prepared at Different Compressions (1 sun illumination)

compression (MPa)	V_{oc} (mV)	J_{sc} (mA cm^{-2})	*ff*	η (%)	estimated surface area ($\times 10^3 cm^2$)
0	480	1.28	0.48	0.51	2.24
10	752	6.53	0.64	3.18	6.62
20	763	7.36	0.58	3.23	8.18
30	805	9.24	0.59	4.39	12.23
40	767	8.68	0.59	3.92	10.51
50	758	7.71	0.61	3.57	8.34
60	735	5.53	0.56	2.31	4.08

3.3. Effect of Mechanical Compression of Nanocrystalline TiO_2 Electrodes on the DSC Performance.

(i). Steady-State J–V Characteristics. The performance of the flexible DSCs on various compressions used in TiO_2 preparation (10–60 MPa) was evaluated on the basis of their steady-state current–voltage characteristics, and Figure 7 shows

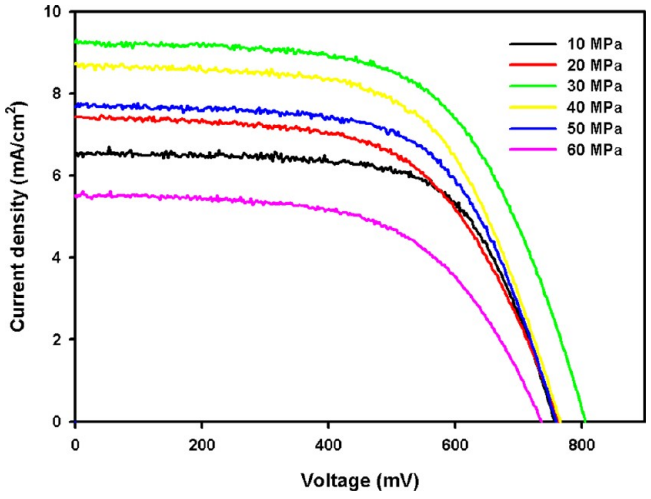

Figure 7. *J–V* characteristics of flexible DSCs constructed by TiO_2 electrodes prepared at different compressions under 1 sun illumination.

the influence of the mechanical compression. Table 1 summarizes the key cell parameters for DSCs as a function of TiO_2 electrode compression. The last column of Table 1 shows the estimated internal surface area of TiO_2 in each case. DSC parameters are significantly influenced by the changes made in applied compression at the TiO_2 electrode preparation stage. J_{sc} and V_{oc} (hence the cell efficiency) increased gradually with increasing compression up to 30 MPa. Further increase of electrode compression caused the drop of the DSC performance, indicating an optimum device performance at 30 MPa compression. This may be due to a combination of factors such as the low density of cracks in the electrode, high internal surface area (i.e., high dye loading), optimized sintering (better transport properties), and low degradation/corrosion behavior of ITO-PEN.

(ii). Incident Photon to Electron Conversion Efficiency (IPCE). In order to study the spectral response of the DSCs, IPCE spectra were recorded by illuminating the cells through

dx.doi.org/10.1021/jp301638p | J. Phys. Chem. C 2012, 116, 19053–19061

the substrate side of dye-coated TiO_2 electrodes (Figure 8). In the present study, the best spectral response was recorded for

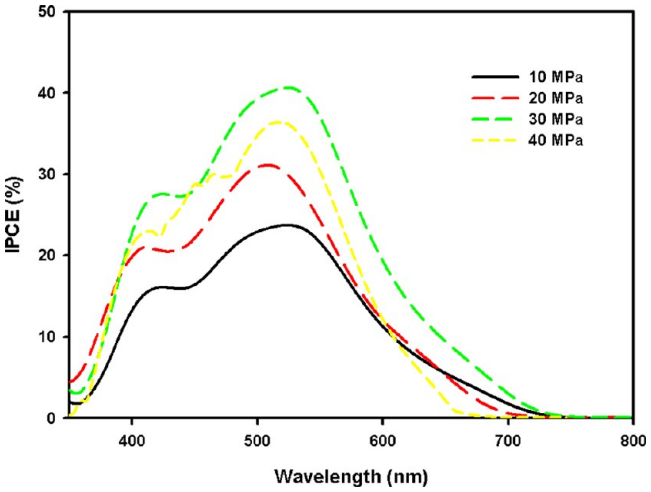

Figure 8. IPCE spectra of DSC prepared using TiO_2 electrodes compressed at different compressions.

the cell made from the electrode compressed at 30 MPa and showed IPCE of 40% at 525 nm. J_{sc} was estimated to be 8.92 mA cm^{-2} by taking into account the integrated IPCE and light absorbance.[24] This value is close to J_{sc} recorded in steady-state $J-V$ measurements for the same DSC (9.24 mA cm^{-2}).

(iii). OCVD Measurements. OCVD measurements were conducted to understand the recombination dynamics of the TiO_2 electrodes of the DSC by means of calculating the effective electron lifetime (τ_{eff}). The photovoltage is recorded at photostationary condition at open circuit. Once the illumination is interrupted, the remaining electrons undergo recombination. The effective electron lifetime relates to the reciprocal of the change of the open-circuit voltage with the time as[25]

$$\tau_{eff} = -\frac{k_B T}{e}\left(\frac{dV_{OC}}{dt}\right)^{-1}$$

where k_B is the Boltzmann constant, T is the absolute temperature, and e is the elementary charge. OCVD data recorded for the cells at the different mechanical compressions are shown in Figure 9. The lifetime decreases several orders of magnitude for all flexible-based DSCs as reported for the glass-based rigid DSCs.[19] The cell made with the electrode compressed at 30 MPa shows the highest electron lifetime, which is in good agreement with $J-V$ and IPCE data. The inset of Figure 9 shows the change of the electron lifetime against the compression at −0.6 V. The electron lifetime peaks at 30 MPa compared to the electrodes prepared at other compressions.

4. CONCLUSIONS

Nanocrystalline TiO_2 electrodes were prepared by the doctor-blade technique using a binder-free titania paste on ITO-PEN substrates at significantly low temperature (140 °C). Electrodes were then compressed in order to improve the interparticle connections and adhesion between the nanoparticles and ITO-PEN substrate. The changes occurring in the electrode texture during compression were studied by electron microscopy. It is evident from the FEG-SEM topographical images that the crack widths for the 30 and 40 MPa compressed TiO_2 electrodes are relatively low. The changes take place in the electrode internal

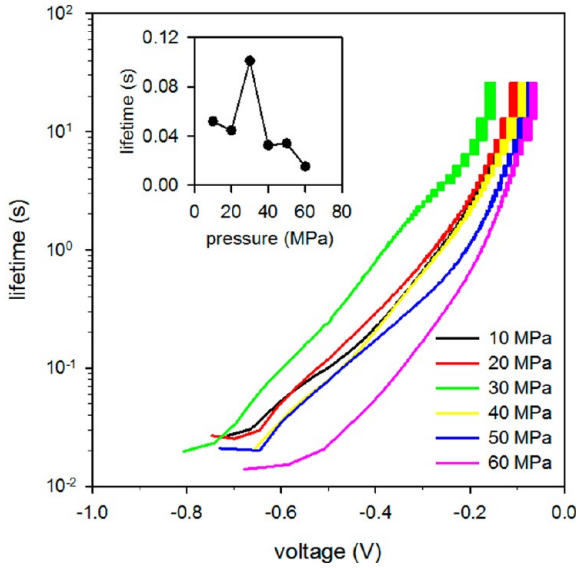

Figure 9. Open-circuit voltage decay measurements of the DSCs made with TiO_2 electrodes prepared at different mechanical compressions. (Inset) Change of effective electron lifetime against compression at −0.6 V.

surface area were estimated by conducting dye adsorption/desorption studies. The highest estimated surface area of nanocrystalline TiO_2 electrode was found when it is compressed at 30 MPa. The electrode prepared at this compression showed the best DSC performance (V_{oc} of 805 mV, J_{sc} of 9.24 mA cm^{-2}, and an overall efficiency of 4.39%).

In order to understand the influence of mechanical compression on TiO_2 electrodes, EIS measurements were performed in the dark for a series of sandwiched cells employing bare nanocrystalline TiO_2 electrodes and Pt counter electrodes in I^-/I_3^- electrolyte. Impedance spectra were characterized under two applied voltage regimes. At relatively positive voltages (from −0.4 to 0 V), TiO_2 electrode is nonconductive and the corresponding impedance spectra describe the charge transfer processes at the counter electrode/electrolyte and ITO/electrolyte interfaces. For simplicity of analysis, the observed three semicircles at this voltage regime are further divided to high-, medium-, and low-frequency domains. These frequency domains were analyzed with the aid of equivalent circuit models. The high-frequency and medium-frequency spectral responses are not commonly seen for glass-based sandwiched cells. The nature of these processes associated with these spectral responses is not completely understood, but we suggest that it may be due to degradation or corrosion undergoing at the ITO-PEN. Cells with nanostructured electrodes compressed at 30 and 40 MPa showed only a minor degradation compared to the other cells. The low-frequency response relates with the recombination dynamics of the cells, and it was analyzed based on the electron lifetime. There is no significant change in the electron lifetime for cells at voltages more positive than −0.4 V. This indicates that the area of the substrate ITO exposed to the electrolyte (i.e., the area of ITO uncoated with TiO_2) is almost similar for all sandwiched cells and was not influenced by the different compressions applied in the TiO_2 electrode preparation step. At voltages negative to −0.4 V, applied compression (in the nanocrystalline TiO_2 electrode preparation) does not significantly influence the electron lifetime. This could be due to the

dx.doi.org/10.1021/jp301638p | J. Phys. Chem. C 2012, 116, 19053−19061

fact that the changes that may take place in recombination (due to the effective TiO_2 area variation at different compressions) are counter balanced by efficient charge collection (as the conductivity of TiO_2 is improved due to better sintering at relatively high compression) and the ITO-PEN degradation/corrosion (at relatively low compression).

OCVD measurements showed that the DSC made by the 30 MPa compressed TiO_2 electrode had the highest decay time, therefore indicating low recombination properties, which is in good agreement with the rest of the results. The findings reported in this work have a direct influence on the development of flexible DSCs. We also believe that our work will have an impact on research in the area of flexible electronics.

AUTHOR INFORMATION

Corresponding Author

*E-mail: U.Wijayantha@lboro.ac.uk.

Notes

The authors declare no competing financial interest.

ACKNOWLEDGMENTS

This work was supported by UK EPSRC, DSTL, Johnson Matthey Plc, and Department of Chemistry, Loughborough University. The authors thank all members of the Renewable Energy Group of the Chemistry Department at Loughborough University for their assistance.

REFERENCES

(1) Li, X.; Lin, H.; Li, J. B.; Li, X. X.; Cui, B.; Zhang, L. Z. *J. Phys. Chem. C* **2008**, *111*, 13744−13753.
(2) Peiris, T. A. N.; Senthilarasu, S.; Wijayantha, K. G. U. *J. Phys. Chem. C* **2012**, *116*, 1211−1218.
(3) (a) Peter, L. M.; Wijayantha, K. G. U. *Electrochim. Acta* **2000**, *45*, 4543−4551. (b) Tennakone, K.; Kumara, G. R. R. A.; Wijayantha, K. G. U.; Kottegoda, I. R. M.; Perera, V. P. S.; Aponsu, G. M. L. P. *J. Photochem. Photobiol. A: Chem.* **1997**, *108*, 175−177.
(4) Wijayantha, K. G. U.; Peter, L. M.; Otley, L. C. *Sol. Energy Mater. Sol. Cells.* **2004**, *83*, 363−369.
(5) Weerasinghe, H. C.; Sirimanne, P. M.; Franks, G. V.; Simon, G. P.; Cheng, Y. B. *J. Photochem. Photobiol. A: Chem.* **2010**, *213*, 30−36.
(6) Zhao, X. C.; Lin, H.; Li, X.; Li, J. B. *Electrochim. Acta* **2011**, *56*, 6401−6405.
(7) Yamaguchi, T.; Tobe, N.; Matsumoto, D.; Arakawa, H. *Chem. Commun.* **2007**, 4767−4769.
(8) (a) Pauchard, L.; Abou, B.; Sekimoto, K. *Langmuir* **2009**, *82*, 513−520. (b) Winnik, M. *Curr. Opin. Colloid Interface Sci.* **1997**, *2*, 192−199. (c) Steward, P. A.; Hearn, J.; Wilkinson, M. C. *Adv. Colloid Interface Sci.* **2000**, *86*, 195−267.
(9) Dragnevski, K. I.; Routh, A. F.; Murray, M. W.; Donald, A. M. *Langmuir* **2010**, *26* (11), 7747−7751.
(10) Jagla, E. A. *Phys. Rev. E.* **2002**, *65*, 046147−046154.
(11) Lee, W. P.; Routh, A. F. *Langmuir* **2004**, *20*, 9885−9888.
(12) Lan, W.; Wang, X.; Xiao, P. *J. Eur. Ceram. Soc.* **2006**, *26*, 3599−3606.
(13) Tinguely, J. C.; Solarska, R.; Braun, A.; Graule, T. *Semicond. Sci. Technol.* **2011**, *26*, 045007−045013.
(14) Tang, C. S.; Shi, B.; Liu, C.; Suo, W. B.; Gao, L. *App. Clay Sci.* **2011**, *52*, 69−77.
(15) (a) Chiu, R. C.; Cima, M. J. *J. Am. Ceram. Soc.* **1993**, *76*, 2769−2777. (b) Sarkar, P.; De, D.; Rho, H. *J. Mater. Sci.* **2004**, *39*, 819−823. (c) Cordelair, J.; Greil, P. *J. Mater. Sci.* **2004**, *39*, 1017−1021.
(16) Aranovich, G. L.; Donohue, M. D. *Colloids Surf. A.* **2001**, *187*, 95−108.
(17) Fabregat-Santiago, F.; Garcia-Belmonte, G.; Mora-Seró, I.; Bisquert, J. *Phys. Chem. Chem. Phys.* **2011**, *13*, 9083−9118.
(18) (a) Lee, K. M.; Chiu, W. H.; Lu, M. D.; Hsieh, W. F. *J. Power Sources* **2011**, *196*, 8897−8903. (b) Chen, H. W.; Lin, C. Y.; Lai, Y. H.; Chen, J. G.; Wang, C. C.; Hu, C. W.; Hsu, C. Y.; Vittal, R.; Ho, K. C. *J. Power Sources* **2011**, *196*, 4859−4864.
(19) Miettunen, K.; Ruan, X. L.; Saukkonen, T.; Halme, J.; Toivola, M.; Huang, G. S.; Lund, P. *J. Electrochem. Soc.* **2010**, *157*, B814−B883.
(20) Sommeling, P.; Späth, M.; Kroon, J.; Kinderman, R.; Van Roosmalen, J. 16th European Photovoltaic Solar Energy Conference and Exhibition, 2000, Glasgow, UK; ECN Solar Energy: The Netherlands.
(21) Fabregat-Santiago, F.; Bisquert, J.; Garcia-Belmonte, G.; Boschloo, G.; Hagfeldt, A. *Sol. Energy Mater. Sol. Cells* **2005**, *87*, 117−131.
(22) Bisquert, J.; Fabregat-Santiago, F.; Mora-Seró, I.; Garcia-Belmonte, G.; Giménez, S. *J. Phys. Chem. C* **2009**, *113*, 17278−17290.
(23) Guillen, E.; Peter, L. M.; Anta, J. A. *J. Phys. Chem. C* **2011**, *115*, 22622−22632.
(24) Dharmadasa, R.; Wijayantha, K. G. U.; Tahir, A. A. *J. Electroanal. Chem.* **2010**, *646*, 124−132.
(25) Bisquert, J.; Zaban, A.; Greenshtein, M.; Mora-Sero, I. *J. Am. Chem. Soc.* **2004**, *126*, 13550−13569.